

# ON DEFORMABILITY OF A ROADBED ACTIVE ZONE UNDER THE INFLUENCE OF A TRAIN WITH INCREASED AXIAL LOADS

Kossov, Valery S., JSC VNIKI, Kolomna, Russia.

Krasnov, Oleg G., JSC VNIKI, Kolomna, Russia.

Nikonova, Natalia M., JSC VNIKI, Kolomna, Russia.

## ABSTRACT

A finite-element model of a railway embankment was developed. Calculations of residual deformations of an active zone of a roadbed using the modified Mohr – Coulomb model in an elastoplastic setting, as well as a comparative evaluation of residual sediments of soil during cyclic loading from wheels

of rolling stock with axle load values of 23.5; 25; 27 and 30 tf were carried out. It is shown that as the loading cycles increase, the dependence of accumulation of residual deformations for clay soils asymptotically tends to a consolidation line of II kind. The intensity of accumulation of residual deformations is higher, the greater are soil moisture and axial load.

**Keywords:** railway embankment, soil models, finite element model, residual deformations, axial load, soil moisture.

**Background.** To determine the rational boundaries for increasing axial loads of rolling stock, it is necessary to know the dependence of intensity of deformation of the roadbed on the level of axial loads.

According to normative documents, a roadbed is designed for an acceptable load of 30 tf and a service life of 100 years [1–3]. At the same time, field observations show that zones of plastic deformation occur on certain sections of a track before the ultimate state occurs in the body and the base of the roadbed under the action of mobile load, weight of soil and weight of a track superstructure.

According to the Center for Inspection and Diagnostics of Engineering Structures, during the last fifteen years the extent of deformed and defective places of the roadbed on the Russian rail network remains at the level of 5,9–8,9%, or 6890–7760 km [4]. Ballast deepenings, sediments and water-bearing pockets are the most widespread deformations. Their share is 73%. All these deformations are associated with a violation of load-bearing capacity of soil of the main site and the active zone of the roadbed.

As a result of long-term operation of the railway track, serious changes in the construction of the roadbed occurred. Clay soils were loaded with powerful layers of sand and gravel. These dumps from draining soils, as shown by the results of a continuous survey of embankments on railways, are not compacted and create a peculiar moisture regime of soils in the upper part of the roadbed.

The layer of accumulated ballast and drainage materials was formed as a result of insufficient load-bearing capacity of clay soils, as the construction norms and rules of SNiP II-39-76, which were in force earlier, regulated location of the ballast prism directly on clay soils. On the construction main platform, plastic deformations formed ballast deepenings – trapezoidal ditches and runways. The moisture of clayey soils in places with these deepenings is 1,2–1,3 times higher than at a level with a drainage area [5].

With this in mind, ensuring strength and permissible value of accumulation of residual deformations of the roadbed with introduction of heavy traffic technology with the use of freight cars with increased axial loads is an actual problem.

**Objective.** The objective of the authors is to consider deformability of a roadbed active zone under the influence of a train with increased axial loads.

The article presents the results of theoretical studies of residual sediments of the roadbed from the impact of freight cars with axial loads up to 30 tf.

**Methods.** The authors use general scientific and engineering methods, Mohr – Coulomb modified

model, mathematical methods, graph construction, simulation.

## Results.

### Selection of a soil model

For reliable prediction of suitability of the roadbed of a railway track, it is necessary to justify the choice of an adequate soil model in accordance with the purpose of the calculations performed. In our case, the problem of comparative estimation of accumulation of residual deformations of the active zone of the railway track from the values of axial loads of rolling stock was solved.

In modern geotechnical calculations, mathematical models of soils of varying degrees of complexity are used. In simpler models, there are fewer input parameters and defining equations are simple and clear. However, the results of the calculation may not correspond to the actual work of soil in a wide range. Advanced, complex calculation models make it possible to describe the behavior of soil more accurately, but request a greater number of different characteristics. Let's consider the most well-known soil models.

To describe the nonlinear behavior of clays for small deformations, the Jardine (R. Jardine) model is used [6]. Unlike the Tresca (Henri Édouard Tresca) model, which is used in calculations taking into account the plastic behavior of the material, when the stresses in the material exceed the specified shear strength, the Jardine model is nonlinearly elastic, which describes the behavior of the material at small deformations.

The D-min model is generally considered as a sectional linear model of strong and weak soils [6]. Such models are characterized by different stiffness at each stage of erection, but they are normalized in such a way that rigidity has a fixed value within the individual stage of erection. It is believed that the elastic modulus decreases, and the Poisson's ratio increases as the Mohr's circle approaches the destruction curve.

The values of the elastic modulus and Poisson's ratio in each section are determined by the relative distance between the Mohr's circle and the destruction curve. The material properties parameters for this model remain constant within each loading stage, that is, they do not need to be recalculated.

The ratio of stresses and deformations for soil materials becomes nonlinear as it approaches the destruction curve, and this can be taken into account by adjustment of the modulus of elasticity of the base. The function of the hyperbolic Duncan – Chang model is used to determine the modulus of elasticity of the base [7]. The stress-strain curve is a hyperbola, and



the modulus of elasticity of the base is a function of tangential stress and stress created by hydrostatic pressure.

The Drucker – Prager model was developed to solve numerical problems arising at the corners of the yield surface of the Mohr – Coulomb model [8]. The yield function is defined in such a way that deviator voltages can increase or decrease depending on the hydrostatic pressure value.

The modified Cam-Clay model is a model of clay materials based on the theory of elastic-plasticity with hardening [8]. To formulate the modified model, all components of effective stresses are used, as well as the nonlinear elastic method and the implicit inverse Euler method. Nonlinear elastic behavior is represented by an increase in the bulk modulus of elasticity at a given pressure. The associated flow law is also applied, and the fracture surface may increase or decrease, which depends on consolidation or decompression. To use the modified Cam-Clay model, the values of the coefficient of initial porosity, natural stresses, and presalting pressures are required.

The hardening soil model (Hardening Soil, Modified Mohr – Coulomb) uses the hyperbolic dependence of deformations on deviator voltages, which more accurately corresponds to the actual behavior of the soil [9–11]. In addition, the modulus of deformation of unloading is introduced into the model when the stresses in the elements decrease.

Analysis of soil models showed that the Hardening Soil model realized in the Plaxis software package can provide the best result for obtaining high accuracy of geotechnical calculations. It requires a significant number of input parameters for physical and mechanical properties of soils obtained during experimental studies.

Taking into account that in this paper the task was to assess deformability of the active zone of the roadbed from the values of axial loads, as well as considerable variety of physicommechanical parameters of soils from which the roadbed of railways is composed, a Mohr – Coulomb model was chosen for calculation, reference data were taken as initial data.

The modified Mohr – Coulomb model is designed to simulate the behavior of granular materials such as soils under the action of a load and is characterized by the following functions:

- the material is strengthened as the pressure increases;
- the model uses isotropic hardening;
- inelastic behavior is usually accompanied by a change in volume;
- the law of plastic flow can be associative and nonassociative;
- material properties may depend on temperature;
- the behavior of soil depends on the hydrostatic pressure.

In this elastoplastic model, there is a yield function in the form of Mohr – Coulomb model, which includes isotropic cohesion hardening / softening. The model uses the potential of plastic flow, which has a hyperbolic form in the meridian plane and has no vertices in the deviator plane. This potential is smooth and allows one to uniquely determine the direction of the plastic flow.

#### The modified Mohr – Coulomb model

To describe the behavior of soil during compression, a hyperbolic yield surface is used [12]. During compression, the plastic flow is considered independent of the effect of pressure

and is determined only by deviator voltages. The soil is considered to be an isotropic material, so that the yield surface can be represented as a function that depends on three invariants of the stress tensor.

For equivalent stresses on pressure:

$$p = -\frac{1}{3} \cdot \sigma : I,$$

where  $\sigma$  – Cauchy stress tensor;  $I$  – unit tensor of the second order.

For equivalent stresses of Mises:

$$q = \sqrt{\frac{3}{2} S : S},$$

where  $S = pI + \sigma$  – stress deviator.

Invariant of deviator stresses:

$$r = \left( \frac{9}{2} S : S : S \right)^{\frac{1}{3}}.$$

In some meridional plane, the Mohr – Coulomb flow surface is represented as:

$$F = R_{mc} q - p \operatorname{tg} \varphi - c = 0,$$

where  $\varphi$  ( $\theta$ ,  $f^\alpha$ ) – angle of internal friction in the meridian plane,  $\theta$  – temperature,  $f^\alpha$  ( $\alpha = 1, 2, \dots$ ) – other field variables;

$c(\bar{\epsilon}^{pl}, \theta, f^\alpha)$  – change in specific hardening (or softening) through specific cohesion;

$\bar{\epsilon}^{pl}$  – equivalent plastic deformation, the speed of which is determined by the equation of plastic work  $c\bar{\epsilon}^{pl} = \sigma : \dot{\epsilon}^{pl}$ ;

$R_{mc}$  – measure of deviator stresses of Mohr – Coulomb, defined by the expression:

$$R_{mc}(\Theta, \varphi) = \frac{1}{\sqrt{3} \cos \varphi} \sin \left( \Theta + \frac{\pi}{3} \right) + \frac{1}{3} \cos \left( \Theta + \frac{\pi}{3} \right) \operatorname{tg} \varphi,$$

where  $\Theta$  – deviator-polar angle [12]:

$$\cos(3\Theta) = \left( \frac{r}{q} \right)^3.$$

The shape of the yield surface in the deviator plane is determined by the angle of internal friction  $\varphi$ :  $0 < \varphi < 90^\circ$ .

The potential of the plastic flow in Mohr – Coulomb model:

$$d\bar{\epsilon}^{pl} = \frac{d\bar{\epsilon}^{pl}}{g} \frac{\partial G}{\partial \sigma},$$

where  $g$  shall be represented in a form of expression

$$g = \frac{1}{c} \sigma : \frac{\partial G}{\partial \sigma};$$

$G$  – plastic flow potential, which is a hyperbolic function in the meridian plane and a smooth elliptic function in the deviator plane:

$$G = \sqrt{(\varepsilon c|_0 \operatorname{tg} \psi)^2 + (R_{mc} q)^2} - p \operatorname{tg} \psi;$$

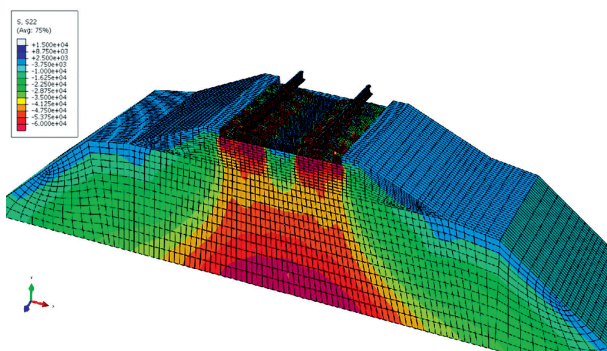
$\psi(\theta, f^\alpha)$  – dilatation angle in the plane  $p - R_{mc} q$  at a high value of the all-round pressure

$$c|_0 \quad c|_{\bar{\epsilon}^{pl}=0, \bar{\epsilon}^{pl}=0}$$

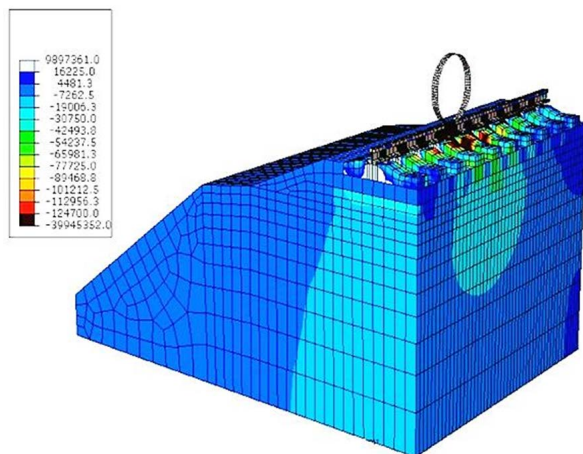
$c|_0 = 0$  – initial specific cohesion;

$\varepsilon$  – eccentricity determining speed of the plastic flow potential.

The presented potential function at large values of the all-round pressure asymptotically tends to a linear plastic flow potential and crosses the hydrostatic pressure axis at an angle of  $90^\circ$ .



**Pic. 1. Finite element model of the upper and lower structure of a railway track.**



**Pic. 2. Stress-strain state of the railway embankment when rolling of wheel of rolling stock.**

**Table 1**

**Characteristics of the materials of upper and lower structures of a track**

Material	Density, kg/m <sup>3</sup>	Young's modulus, Pa	Poisson's ratio
Steel (rail)	7800	210e9	0,30
Concrete (sleeper)	3000	30e9	0,25
Rubber (gasket)	1300	9e8	0,45
Crushed stone	2500	254e6	0,27
Sand	2500	100e6	0,40
Ground	2000	4e7	0,40

*In the deviatorial plane, the plastic flow potential is continuous and smooth [13]:*

$$R_{mw}(\theta, e) = \frac{R_1}{R_2 + R_3} K_{mc},$$

where  $R_1 = 4(1 - l^2) \cos^2 \theta + (2e - 1)^2$ ;

$$R_2 = 2(1 - e^2) \cos \theta;$$

$$R_3 = (2e - 1) \sqrt{(1 - e^2) \cos^2 \theta + 5e^2 - 4e};$$

$$K_{mc} = R_{mc} \left( \frac{\pi}{3} \varphi \right) = \frac{(3 - \sin \varphi)}{6 \cos \varphi};$$

$\theta$  – deviator polar angle;

$e$  – a parameter representing the degree of difference from the circular shape for the yield surface in the deviator plane as the ratio of tangential stresses along the extension meridian ( $\theta = 0$ ) to tangential

stresses along the meridian of compression ( $\theta = \frac{\pi}{3}$ ). The parameter  $e$  depends on the angle of internal friction  $\varphi$  and is calculated by equating the plastic flow potential to the flow surface in the deviator plane:

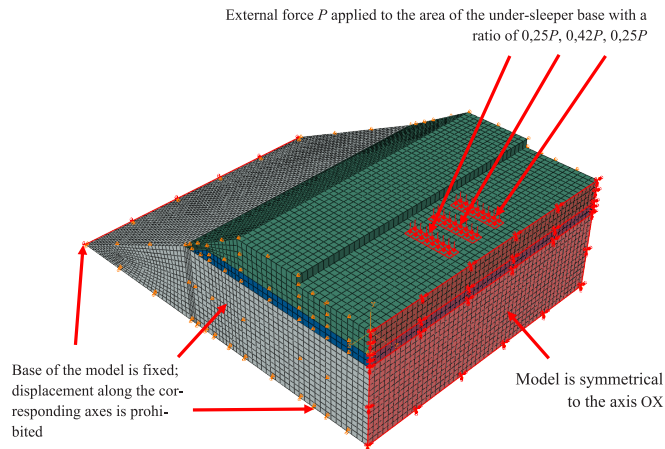
$$e = \frac{3 - \sin \varphi}{3 + \sin \varphi}.$$

Because of convexity of the material and smoothness of the elliptic function, the following condition must be satisfied:  $\frac{1}{2} < e \leq 1$ .

When the angle of internal friction  $\varphi$  is equal to the dilatation angle  $\psi$ , the parameter  $e$  is small. The plastic flow in the meridional plane is close to the associated one.

In the general case, the plastic flow in the meridional plane is unassociated. The plastic flow in the deviator plane always remains unassociated.





**Pic. 3. Finite-element model of an under-sleeper base with boundary conditions and a scheme for applying vertical loads from three neighboring sleepers.**

**Table 2**

**Initial data of models**

No. of a model	Axle load, tf	Soil fluidity indicators		
		Soil fluidity indicators I	Specific cohesion of soil, c*, kPa	Angle of internal friction, $\varphi^{**}$ , deg.
1	23,5	$I_1 = 0,25$	31	24
2		$I_2 = 0,45$	28	22
3		$I_3 = 0,6$	25	19
4	27	$I_1 = 0,25$	31	24
5		$I_2 = 0,45$	28	22
6		$I_3 = 0,6$	25	19
7	30	$I_1 = 0,25$	31	24
8		$I_2 = 0,45$	28	22
9		$I_3 = 0,6$	25	19

\*c – soil fluidity indicators (Cohesion Yield Stress); \*\* $\varphi$  – angle of internal friction (Friction / Dilation Angle).

**Finite-element model**

To study the residual deformations of the roadbed from the values of axial loads, a finite-element model of the upper and lower structure of the track was developed (Pic. 1). It includes rails and sleepers consisting of R65 rails, intermediate rail fasteners, a ballast layer 0,4 m thick, a sand cushion 0,2 m thick and a roadbed with standard parameters. The roadbed serves as a base of track superstructure and perceives load from it and rolling stock. The calculated embankment and the design of track superstructure are designed in accordance with the requirements of SP 119.13330.2012, SP 32-104-98 [2, 3].

The scheme of the model of the railway embankment is symmetrical relative to the axis OX, stress-strain state of the embankment during rolling of wheel of rolling stock is shown in Pic. 2.

Considering the fact that we are analyzing the stress-strain state of the under-sleeper base, axial

load in the model was set as the external force P, distributed on three adjacent sleepers (under-sleeper base) in a ratio of 0,25P, 0,42P, and 0,25P. This procedure excludes the expenditure of computer time for calculating the stress-strain state of the elements of rails and sleepers, reducing the counting time.

Since the stress state in the roadbed, caused by the impact of rolling stock, reduces significantly with increasing depth from the sole of the sleeper, the active zone of the road bed 2 m deep from the sole was considered in the model.

Pic. 3 shows the finite-element model of a 5 m long section (roadbed, ballast) with boundary conditions and a scheme for applying vertical loads. The characteristics of the materials used in the model are given in Table 1.

The model requires the input of the following parameters: modulus of elasticity E, Poisson's ratio, angle of internal friction and dilatancy. The last two serve to determine the state of fluidity. The formulation of the defining equations assumes effective parameters of the angle of internal friction  $\varphi$  and adhesion c.

In the calculations, the effect on deformability of the active zone of the roadbed, the forces transferred from wheels to rails and soil moisture were studied.

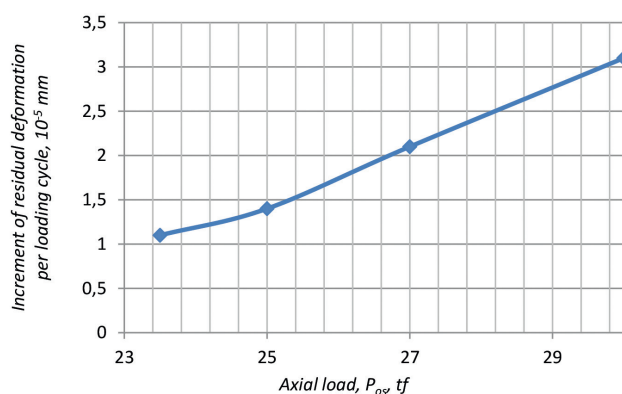
To estimate the effect of the axle load of a wheel set and soil moisture on deformation of a railway

**Table 3**

**Change in residual deformations of soil**

Axle load, tf	E <sub>a</sub> , MPa		
	40	60	80
23,5	0,138	0,112	0,075
30	0,213	0,157	0,100





**Pic. 4. Dependence of change in increment of residual sediments of soil at  $E_g = 60$  MPa,  $I < 0,25$  on values of axial loads after 100 cycles of loading.**

embankment, six calculation models were considered (Table 2). The calculation was carried out for a roadbed composed of loam with a coefficient of porosity  $e = 0,65$  [14]. The initial data for soil was selected on the basis of the analysis of the main type of the most common soils on the territory of Russia. As initial data of vertical forces during the simulation, the loads received during the dynamic tests of an experimental train including freight cars with axial loads of 23,5, 25, 27 and 30 tf were taken [15]. The values of fluidity index, angle of internal friction, and specific cohesion for loam were selected from the reference book [14].

The physical and mechanical characteristics of soils composing the under-sleeper base are shown in Table 2.

As a result of calculations, the dependences of the change in residual deformations of the main area of the roadbed on the values of axial loads and soil moisture were obtained with a change in the fluidity index from  $I < 0,25$  to  $0,5 < I < 0,75$ .

Analysis of the curves of the changes in the position of the main area of the roadbed during cyclic loading showed at the initial moment of observation an abrupt change in sediment for all the options considered (compaction, moisture and axial loads). The difference consists in the values of the initial change in residual sediments and in the intensity of their accumulation before the onset of consolidation. The values of the changes in the residual deformations of soil with a different deformation modulus are presented in Table 3.

With further cyclic loading, the intensity of accumulation of sediments decreased and decreased monotonically with different values of the increment of sediments, depending on the values of axial loads, the modulus of deformations, and the physico-mechanical characteristics of soil.

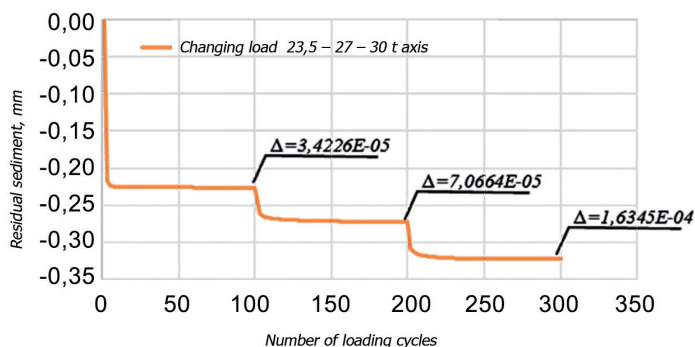
After 100 cycles of loading, the increment of residual sediments had values in the range of  $10^{-5}$ – $10^{-6}$  mm. With a further increase in the number of loading cycles, it decreased to  $10^{-7}$ – $10^{-8}$  mm. The intensity of accumulation of residual deformations of clay soils depended on the values of axial loads, the degree of compactness of soil and soil moisture.

The nature of the change in increments of the residual sediments of the railway embankment after 100 cycles of axial loads: 1) 23,5 tf; 2) 25 tf; 3) 27 tf; 4) 30 tf (soil – loam);  $c = 31$ ,  $\varphi = 22^\circ$ , the fluidity index  $I < 0,25$  (dry soil) is illustrated in Pic. 4.

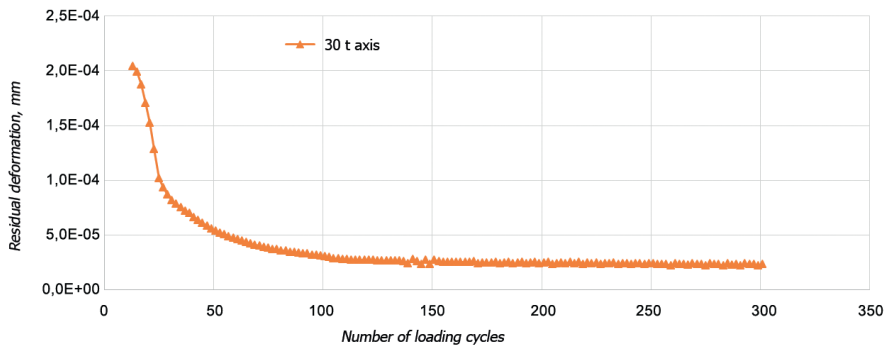
Analysis of simulation results showed that the increment of residual sediments during compaction of dry soils increases almost linearly along with the values of axial loads.

Pic. 5 shows changes in the dependence of increments of residual deformations with a consecutive increase in axial loads and cyclic loading on the 3D model of an under-sleeper base with a sequence of 100 loading cycles for each load value.

With an axial load value of 23,5 tf at the initial moment in case of cyclic action a jumplike deformation characteristic of clay soils occurs. For the case of loams with  $E_g = 40$  MPa, specific cohesion



**Pic. 5. Nature of change in the increments of residual deformations of the main area of roadbed with a consequent increase in axial loads with a sequence of 100 cycles of loading. Soil fluidity  $0,25 < I \leq 0,5$ ; specific cohesion  $c = 28$  kPa; angle of internal friction  $\varphi = 22^\circ$ .**

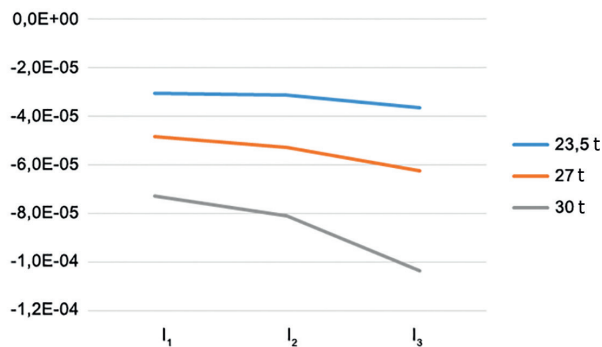


**Pic. 6. Nature of change in the increments of residual deformations of the main area of the roadbed under cyclic action with axial load  $P_{ax} = 30$  tf with fluidity index  $I < 0,25$ .**

**Table 4**

**Change in the increments of residual deformations of the main area of the roadbed under cyclic action from axial loads  $P_{ax} = 23,5; 27; 30$  tf at the fluidity index  $I_1 < 0,25; 0,25 < I_2 \leq 0,5; 0,5 < I_3 \leq 0,75$**

Axle load, tf	Soil moisture		
	$I_1$	$I_2$	$I_3$
23,5	-3,0617E-05	-3,1316E-05	-3,6438E-05
27	-4,8312E-05	-5,2969E-05	-6,2282E-05
30	-7,2876E-05	-8,1025E-05	-1,0361E-04



**Pic. 7. Change of residual deformations of the main area of the roadbed under cyclic action with axial loads  $P_{ax} = 23,5; 27; 30$  tf with fluidity indicators  $I_1 < 0,25; 0,25 < I_2 \leq 0,5; 0,5 < I_3 \leq 0,75$ .**

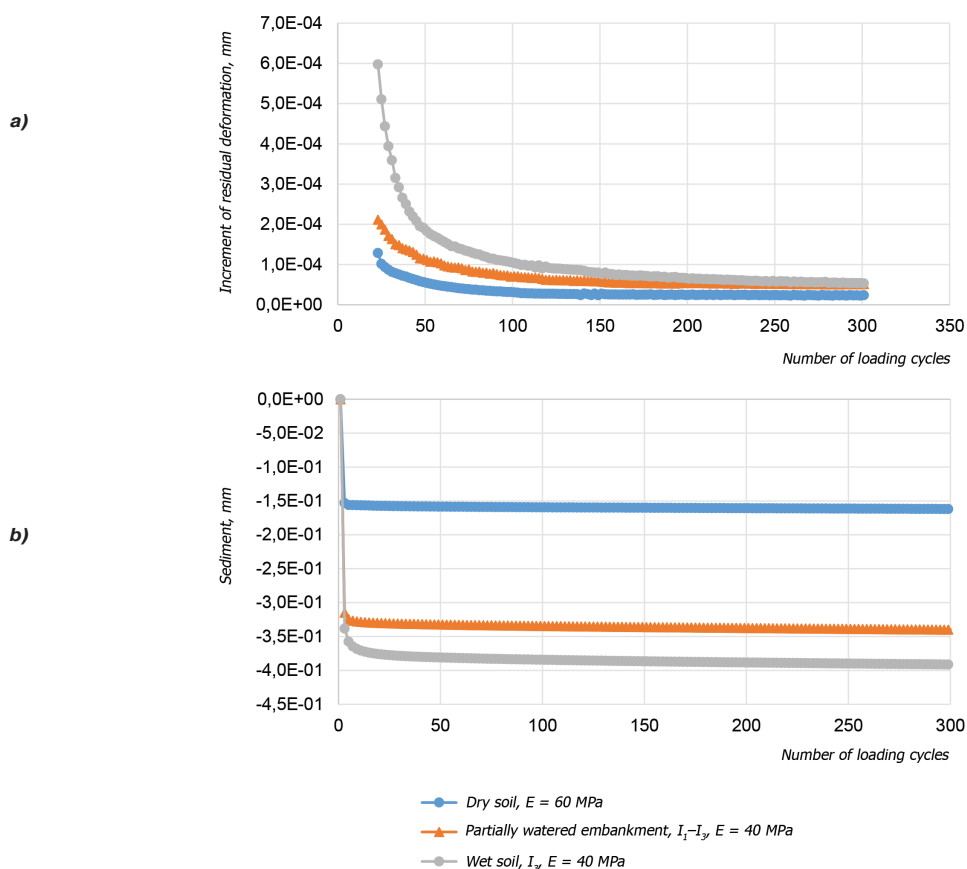
$c = 28$  kPa, angle of internal friction  $\phi = 22^\circ$ , at values of the fluidity index  $0,25 < I \leq 0,5$ , its residual deformation value was up to 0,22 mm. With further cyclic loading, the increment of residual deformations decreased monotonically. With an increase in the number of load cycles, the dependence of the increment of residual deformations asymptotically approached the state of consolidation of the soil. An increase in axial load up to 27 tf determined an additional spasmodic increase in sediment during the first loading cycles, after which the sediment increment stabilizes at a level of  $10^{-5}$  mm, tending to the consolidation state. With an increase in the axial load up to 30 tf, the nature of the change in the residual sediment was similar.

It should be noted that the intensity of soil sediment change, their total value, and, consequently, the degree of compaction, will be maximum at the

highest value of the axial load. The nature of the intensity of changes in soil deformations during cyclic action up to 300 cycles with an axial load of  $P_{ax} = 30$  tf with a fluidity index  $I < 0,25$  is shown in Pic. 6.

Dependence of the change in residual sediments of soil under cyclic loading by an axial load of 30 tf has a character of a monotonically decreasing curve asymptotically approaching the limiting state of compaction – consolidation of clay soils of II kind.

Modeling of the change in the rate of accumulation of residual deformations of soils from the change in the fluidity index within the limits  $I \leq 0,25$  to  $0,5 < I \leq 0,75$  over the entire volume of the soil is carried out, which is characteristic of the exit of the railway track from winter or periods of heavy precipitation. The values of the increments of residual deformations of the soil for different moisture and axial loads are presented in Table 4 and in the form of graphs in Pic. 7.



**Pic. 8. Change in the increments of residual deformations (a) and residual deformations (b) of the main site of the roadbed under cyclic action with axial loads of  $P_{ax} = 30$  tf with different soil moisture content of the under-sleeper base.**

From the obtained dependences it is established that the change in the increments of residual deformations increases with increasing axial loads and an increase in moisture. In all cases, a gradual decrease in incremental values with an asymptotic approach to the limiting state compaction – consolidation of clay soils of II kind is typical for all cases.

For a more detailed study of the nature of the change in residual deformations at a soil fluidity index of  $0,5 < I \leq 0,75$  and cyclic action with an axial load of 30 tf, calculations of the change in residual deformations are performed.

Studies of the effect of watering the soil in a local zone, characteristic of wet spills, have also been carried out. To do this, the finite-element 3D model of the under-sleeper base is modified: the main part of the soil has a moisture content  $I \leq 0,25$ , and in the local zone under three adjacent sleepers the soil has a moisture content with a fluidity index of  $0,5 < I \leq 0,75$ . The model with watering of the soil in the local zone is shown in Pic. 8.

The results of modeling the change in residual deformations for watered, partially watered in a local area and for dry soil under cyclic loading by an axial load of 30 tf based on 300 cycles are shown in Pic. 8.

The greatest value of deformation from the moment of the beginning of cyclic loading to achievement of consolidation was reached at loads of 30 tf and a fluidity index of  $0,5 < I < 0,75$ .

On an embankment composed of loam with a deformation modulus  $E_g = 60$  MPa and a fluidity index  $I \leq 0,25$ , the residual deformation until reaching a state close to consolidation did not exceed 0,15 mm, with a soil fluidity index of  $0,5 < I < 0,75$  at  $E_g = 40$  MPa, the residual deformation was 0,45 mm.

When watering the soil in a local zone, the value of the residual deformation was 0,35 mm, taking an intermediate value, which can be explained by an increased resistance to residual deformation of adjacent non-watered sections of the roadbed.

On the basis of the dependences obtained, it is established that the moisture state of the soils of the under-sleeper base has a significant effect on the accumulation of residual deformations.

#### Conclusion.

1. A finite-element 3D model of a three-layer railway embankment was developed using the modified Mohr – Coulomb model, taking into account the behavior of soil in the elastoplastic zone. The process of accumulation of residual deformations under cyclic loading by axial loads of 23,5, 25, 27 and 30 tf with change of the soil fluidity index from  $I < 0,25$  to  $0,5 < I < 0,75$  was performed, with soil watering in the period of transition of railway track from winter season or a period of heavy precipitation, with partial watering in local areas, characteristic of wet spills.

2. As a result of modeling the process of filling residual deformations under cyclic loading with





axial loads of 23,5; 25; 27 and 30 tf, it was established that for clay soils in the entire range of loads and moisture examined the nature of accumulation of residual deformations had characteristic phases:

- in the initial period (phase 1), the change and increment of residual deformations had a discontinuous character, while the higher was the axial load and moisture, the higher were the values of increments of residual deformations;
- the second phase: the transition zone from the intensive accumulation of residual deformations to a monotonically decreasing one;
- the third phase: the zone of minimum increments of residual deformations, at which the incremental curve asymptotically tends to the state of limiting compaction–consolidation of soils of II kind.

3. On an embankment composed of loam with a deformation modulus  $E_g = 60$  MPa and a fluidity index  $I \leq 0,25$ , the residual deformation until reaching a state close to consolidation did not exceed 0,15 mm, with a soil fluidity index of  $0,5 < I < 0,75$  and a deformation modulus  $E_g = 40$  MPa, the residual deformation was 0,45 mm.

When watering the soil in the local zone, the value of the residual deformation was 0,35 mm, occupying an intermediate value, which can be explained by the increased resistance of adjacent non-watered sections of the roadbed.

4. In the entire range of the axial loads and moisture in question, no limit state has been reached, at which it is possible to shift the soil masses along the slip lines. For all the cases considered, soil consolidation was observed, taking into account both the ball and deviator stresses in the model.

5. To verify the developed procedure for determining residual deformations, it is necessary to monitor accumulation of residual deformations in the areas of controlled operation of freight cars with axle loads of 25 and 27 tf.

## REFERENCES

1. On the strategy for development of rail transport in the Russian Federation until 2030. Order of the Government of the Russian Federation of 17.06.2008 № 877 r [O strategii razvitiya zheleznodorozhnogo transporta v Rossiiskoi Federatsii do 2030 goda. Rasporyazhenie pravitelstva RF ot 17.06.2008 № 877 r].
2. SP 119.13330.2012. Railways of gauge 1520 mm. The updated version of SNiP 32-01-95 (with amendment No. 1) [SP 119.13330.2012. Zheleznye dorogi kolei 1520 mm. Aktualizirovannaya redaktsiya SNiP 32-01-95 (s izm. No. 1)]. Moscow, 2012, 52 p.
3. SP 32-104-98. Designing of a roadbed of railways of a track of 1520 mm [SP 32-104-98. Proektirovanie zemlyanogo polotna zheleznykh dorog kolei 1520 mm]. Moscow, 1999, 90 p.

4. Lebedev, A. V. Analysis of the state of a roadbed [Analiz sostoyaniya zemlyanogo polotna]. Put' i putevoe hozyaistvo, 2017, Iss. 8, pp. 8–11.

5. Guidelines for determining the physical and mechanical characteristics of ballast materials and soils of PMI-36 roadbed. Approved by the department of tracks and structures of the Ministry of Railways of the Russian Federation of 30.01.2004 [Rukovodstvo po opredeleniyu fiziko-matematicheskikh harakteristik ballastnykh materialov i gruntov zemlyanogo polotna PMI-36. Urv. departamentom puti i sooruzhenii MPS RF ot 30.01.2004].

6. Dalidovskaya, A. A. Design models of soils [Raschetnye modeli gruntov]. Scientific leader V. G. Pastukhov. In: Design, construction and operation of transport facilities: Proceedings of 72<sup>nd</sup> student scientific-technical conference. Belarusian National Technical University. Minsk, BNTU, 2016, pp. 19–24.

7. Duncan, J. M., Chang, Chin-Yung. Nonlinear Analysis of Stress and Strain in Soils. Journal of the Soil Mechanics and Foundations Division, 1970, Vol. 96, Iss. 5, pp. 1629–1653.

8. Development of a verification report on the use of the software package ABAGUS for solving the problems of the building profile: scientific and technical. report. Vol. 1 [Razrabotka verifikatsionnogo otcheta po ispolzovaniyu programmnoy kompleksa ABAGUS dlya resheniya zadach stroitel'nogo profilya: nauchno-tehnicheskiiy otchet. T. 1]. Moscow State University of Civil Engineering. Moscow, 2013, 268 p.

9. Strokova, L. A. Determination of parameters for numerical simulation of soil behavior [Opredelenie parametrov dlya chislennogo modelirovaniya povedeniya gruntov]. Tehnologiya i tehnika geologo-razvedochnykh rabot, 2008, Iss. 1, pp. 69–74.

10. Brinkgreve, R. B. J., Vermeer, P. A. A new approach to softening plasticity. Proceeding of the 5<sup>th</sup> International Symposium on Numerical Models in Geomechanics (Switzerland), 1995, pp. 193–202.

11. Schanz, T., Vermeer, P. A., Bonnier P. G. The Hardening-Soil Model: Formulation and verification. In: Beyond 2000 in Computational Geotechnics. Balkema, Rotterdam, 1999, pp. 281–290.

12. Chen, W. F., Han, D. I. Plasticity for Structural Engineers. Springer-Verlag., New York., 1988, 606 p.

13. Menetrey, Ph., Willam, K. J. Triaxial Failure Criterion for Concrete and its Generalization. *ACI Structural Journal*, 1995, Vol. 92, Iss. 3, pp. 311–318.

14. Dydyshko, P. I. Design of a roadbed of a railway track: Reference guide [Proektirovanie zemlyanogo polotna zheleznodorozhnogo puti: Spravochn. posobie]. Moscow, Intext publ., 2011, 152 p.

15. Comprehensive comparative studies of the impact on the infrastructure of cars with an axial load of up to 30 tf on Golutvin–Ozery sections of Moscow railway: report on the research: 1–6–17 [Kompleksnie sravnitelnie issledovaniya vozdeystviya na infrastrukturu vagonov s osevoi nagruzkoi do 30 ts na uchastkah Golutvin–Ozery Moskovskoi zh.d.: otchet o NIR: 1–6–17]. VNIKTI JSC. Kolomna, 2017, 87 p.

Information about the authors:

**Kossov, Valery S.** – D.Sc. (Eng), professor, general director of JSC VNIKTI, Kolomna, Russia, vnikti@ptl-kolomna.ru.

**Krasnov, Oleg G.** – Ph.D. (Eng), head of the department of JSC VNIKTI, Kolomna, Russia, +7(496) 618-82-48.

**Nikonova, Natalia M.** – engineer-programmer of I category of JSC VNIKTI, Kolomna, Russia, vnikti@ptl-kolomna.ru.

Article received 13.07.2018, accepted 24.08.2018.

Work was made within the project RFFI 17-20-01088.